

UDC 538.971

DOI: 10.15372/CSD2020245

# Investigation of the Structural Features and Capacitive Parameters of Carbon Materials Based on Carbonized Rice Husk

Z. A. MANSUROV<sup>1,2</sup>, A. P. NIKITIN<sup>3</sup>, G. YU. SIMENYUK<sup>3</sup>, YU. A. ZAKHAROV<sup>3</sup>,  
V. V. PAVLENKO<sup>1,2</sup>, Z. R. ISMAGILOV<sup>3</sup>

<sup>1</sup>*Al-Farabi Kazakh National University,  
Almaty, Kazakhstan*

*E-mail: galina-simenyuk@yandex.ru*

<sup>2</sup>*Institute of Combustion Problems,  
Almaty, Kazakhstan*

<sup>3</sup>*Federal Research Center of Coal and Coal Chemistry, Siberian Branch of the Russian Academy of Sciences,  
Kemerovo, Russia*

(Received February 11, 2020)

## Abstract

Porous carbon materials with a specific surface area of 1200–1500 m<sup>2</sup>/g were obtained by carbonization of rice husks at 500 °C, followed by subsequent activation using potassium hydroxide at a temperature of 700, 800, 900 °C, and studied by means of Raman spectroscopy and electrochemical methods. It was established that mechanical activation of rice husks makes it possible to increase the specific surface area (to 2315 m<sup>2</sup>/g) and the volume of micropores (to 0.84 cm<sup>3</sup>/g) in the carbon material. As a result, an increase in electrical capacity and a decrease in the internal resistance of supercapacitor cells with electrodes based on them are achieved.

**Keywords:** carbon materials, rice husks, carbonation, electrochemical properties

## INTRODUCTION

Porous carbon materials (PCM) find broad application as adsorbents, supports for catalysts and electrode materials [1–3]. The major sources of obtaining highly porous activated carbon materials are fossil brown and black coal, wood, wood charcoal, peat, etc. A tendency is observed to use the wastes of plant raw material from agricultural production as precursors (fruit seeds, nut shells, husk of grain crops, straw, corn cobs, etc.) [4–6].

Special attention should be paid to a cheap and available renewable raw material – rice husk. The world amount of rice production is more than 500 million t per year, and rice husk is formed as the wastes in the amount of about

140 million t [7]. Rice husk is usually used as a cheap source of energy; it is burnt in the fields or stored as wastes in enormous amounts, which has a negative effect on the environment.

The major components of rice husk are cellulose, hemicellulose, lignin, and mineral components (mainly silicon compounds); their content depends on rice sort, climatic conditions, the chemical composition of soil, the methods of land cultivation and irrigation, fertilizers and other conditions.

In this connection, the development of methods to obtain PCM based on rice husk is urgent [8–12] because this allows us not only to make materials with unique adsorption and capacitive properties on the basis of cheap and

available raw material but also to solve the problem of waste utilization thus promoting conservation of the environment.

The parameters of porous structure (the size, volume and structure of pores) may be regulated within a broad range by varying the conditions of carbonization, activation and removal of silicon oxide during obtaining PCM. In the case of chemical activation, which is carried out at lower temperatures than physical activation, the reagents used to increase porosity are potassium hydroxide, potassium carbonate, zinc chloride, phosphoric acid, *etc.* [2, 7, 13, 14]. However, the use of such activators as phosphoric acid, zinc chloride and some others requires additional leaching of residual silicon oxide.

Because of this, especially interesting is the optimization of the technology of highly porous activated coal from rice husk by uniting the process of silicon oxide removal and chemical activation. This is achieved by using potassium hydroxide as the activator: at high temperature, this compound not only promotes an increase in the specific surface of the formed carbon material but also interacts with silicon oxide with the formation of water-soluble potassium silicate. Subsequent dissolution of potassium silicate in cold water is accompanied by an increase in porosity [12, 13, 15].

Due to the highly developed structure of meso- and micropores, these materials are of interest for use as the electrodes in the systems of energy accumulation and transfer. Micropores provide high porosity for the adsorption of electrolyte ions, which leads to high specific capacitance, while mesopores in combination with macropores promote the formation of transport channels for electrolyte ions. A three-dimensional multiscale structure simplifies the penetration of the electrolyte and ion diffusion, thus improving the access of electrolyte ions to the electrode. High chemical stability and good electrical conductivity provide excellent stability during multiple potential cycling. The main factors affecting the characteristics of the materials of electrodes in supercapacitors (SC) are specific surface [16], pore size distribution [17], specific resistance [18, 19], and functional groups on the surface [20].

However, the use of the excess amount of potassium hydroxide as the activating agent leads first of all to an increase in the volume of macropores and large mesopores, which causes a decrease in Van der Waals forces inside the pores and has a negative effect on capacitance charac-

teristics; second, this causes a decrease the density of the material as a result of more rigid activation conditions, which inevitably causes a decrease in volume capacitance, the most practically significant characteristic in the area of miniaturization of electronics; third, this causes a decrease in the total yield of carbon material, which leads to an inevitable increase in the net cost of the production of capacitors.

In this connection, it is most relevant to investigate the processes of obtaining and properties of PCM based on carbonized rice husk treated with the use of an optimal amount of activator (potassium hydroxide) because this allows obtaining carbon material under softer conditions, in a high yield, with prevailing microporosity combining a moderate fraction of mesopores, which would provide simplified charge propagation at a high scanning rate.

The goal of the present work was to study the effect of the conditions of chemical and mechanical activation of carbonized rice husk on the structural features of the obtained carbon materials and on the capacitance characteristics of the electrodes of SC on this basis.

## EXPERIMENTAL

### Materials

Highly porous activated carbon materials based on rice husk (RH) collected in the Almaty Region of the Republic of Kazakhstan were chosen as the object of investigation. The carbon materials were obtained at the Institute of Combustion Problems (Almaty, the Republic of Kazakhstan) according to the following procedure: rice husk was preliminarily purified, dried and carbonized at 500 °C in the atmosphere of nitrogen for 40 min (RH-C-500). Then carbonized husk RH-C-500 was mixed with KOH at a mass ratio of 2 : 1, placed in a crucible made of stainless steel and activated in the atmosphere of nitrogen at a temperature of 700, 800 and 900 °C for 1 h. The resulting mixture was washed with cold water to achieve the neutral medium (pH) by separating from the liquid phase by decanting, and then dried at 110 °C for 1 h. The samples of the activated carbon material obtained as a result of chemical activation with potassium hydroxide (RH-CA-700, RH-CA-800 and RH-CA-900) were studied using different methods. For comparison, RH(M)-CA-800 sample was prepared on the basis of rice husk after preliminary mechanical activa-

tion (comminuted to the size fraction of 500  $\mu\text{m}$ ); this sample was subjected to carbonization and activation under the conditions similar to those for the RH-CA-800 sample.

### Physicochemical investigations

Specific surface and pore volume were estimated with the help of Autosorb-1 sorbometer (Quantachrome instruments, UK) according to Brunauer–Emmett–Teller method (BET) relying on the isotherms of low-temperature (77 K) sorption of nitrogen. Before analysis, carbon materials were degassed at 350  $^{\circ}\text{C}$  for 12 h in vacuum.

Investigation of the samples by means of Raman spectroscopy (RS) was carried out with the help of a Renishaw InVia Basis spectrometer (Renishaw, UK) with the excitation wavelength of 514.5 nm and exposure for 90 s per each spectrum.

### Electrochemical measurements

Electrochemical measurements were carried out in a two-electrode cell of symmetrical design with graphite current collectors with the help of a Parstat 4000 potentiostat-galvanostat-impedance meter (Princeton Applied Research, USA) using aqueous solutions of 1 M  $\text{H}_2\text{SO}_4$  or 6 M KOH as electrolytes, and a porous polypropylene membrane PORP-A1 (Russia) as a separator.

The curves of cyclic voltammetry (CVA) were recorded within the potential window from  $-1$  V to  $+1$  V with the potential scanning rates 10, 20, 40 and 80 mV/s.

Measurements by means of galvanostatic charging-discharging were carried out with the charging current  $+10$  mA, discharging current  $-10$  mA, time of discharging/charging 10 s, current density 0.5 A/g (calculated for the mass of two electrodes). On the basis of the data obtained, we calculated specific capacitance and internal resistance.

Impedance measurements were carried out in the potentiostatic mode within a frequency range of  $10^{-2}$  to  $10^4$  Hz.

The procedure for the calculation of capacitance characteristics was reported in [21–23].

## RESULTS AND DISCUSSION

The porous material obtained as a result of rice husk carbonization is characterized by not very large specific surface area (149  $\text{m}^2/\text{g}$ ) and contains a substantial amount of amorphous silicon oxide. Chemical activation of carbonized husk with the help of KOH causes a substantial increase in specific surface and porosity, especially after the removal of silica. After activation at a temperature of 800  $^{\circ}\text{C}$ , specific surface and total pore volume reach the maximal values; further temperature rise to 900  $^{\circ}\text{C}$  causes a decrease in porosity (Fig. 1). So, 800  $^{\circ}\text{C}$  is the optimal temperature for the high-temperature activation of carbonized rice husk with the help of potassium hydroxide. It was established that preliminary mechanical activation of rice husk allows an additional increase in

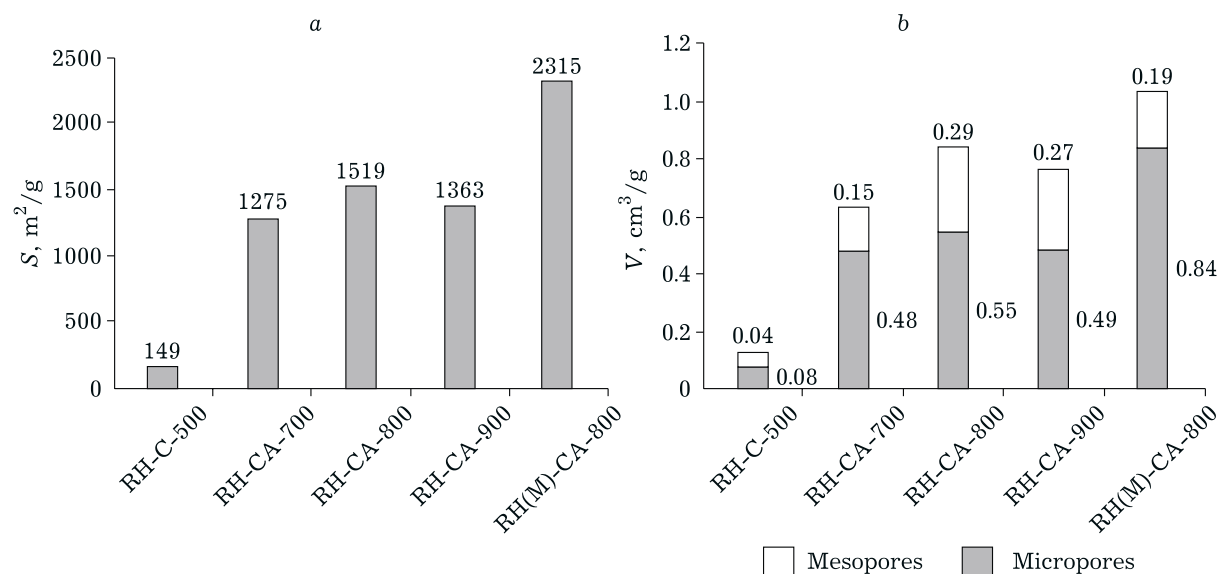


Fig. 1. Texture characteristics of carbon materials based on rice husk: a – specific surface area; b – volumes of meso- and micropores.

the specific surface area and micropore volume by a factor of approximately 1.5.

The Raman spectra of the samples are shown in Fig. 2. One can see that the behaviour of the curves in the spectrum of carbonized rice husk (RH-C-500) (see Fig. 2, *a*) changes sharply after its mechanical and chemical activation (see Fig. 2, *b*–*e*). The high intensity of luminescence background (see Fig. 2, *a*) is evidence of the presence of not only C–C bonds but most probably also oxygenated functional groups in the structure of the material. Analysis of the Raman spectra of the first order involves their decomposition according to the 5V model (five vibra-

tions described by pseudo-Voigt functions), followed by the calculation of numerical characteristics to describe the degree of imperfection of the carbon framework of materials under investigation.

Within the spectra range of 900–1900  $\text{cm}^{-1}$ , the following bands were assigned to the basic vibrations of carbon atoms included in various molecular formations [24–27]:

D4-band  $\sim 1200 \text{ cm}^{-1}$  (mixed structure involving  $sp^3$ - $sp^2$ -hybrid carbon);

D-band  $\sim 1360 \text{ cm}^{-1}$  ( $sp^3$ -atoms of carbon in a diamond-like structure or the presence of heteroatoms in the graphite plane);

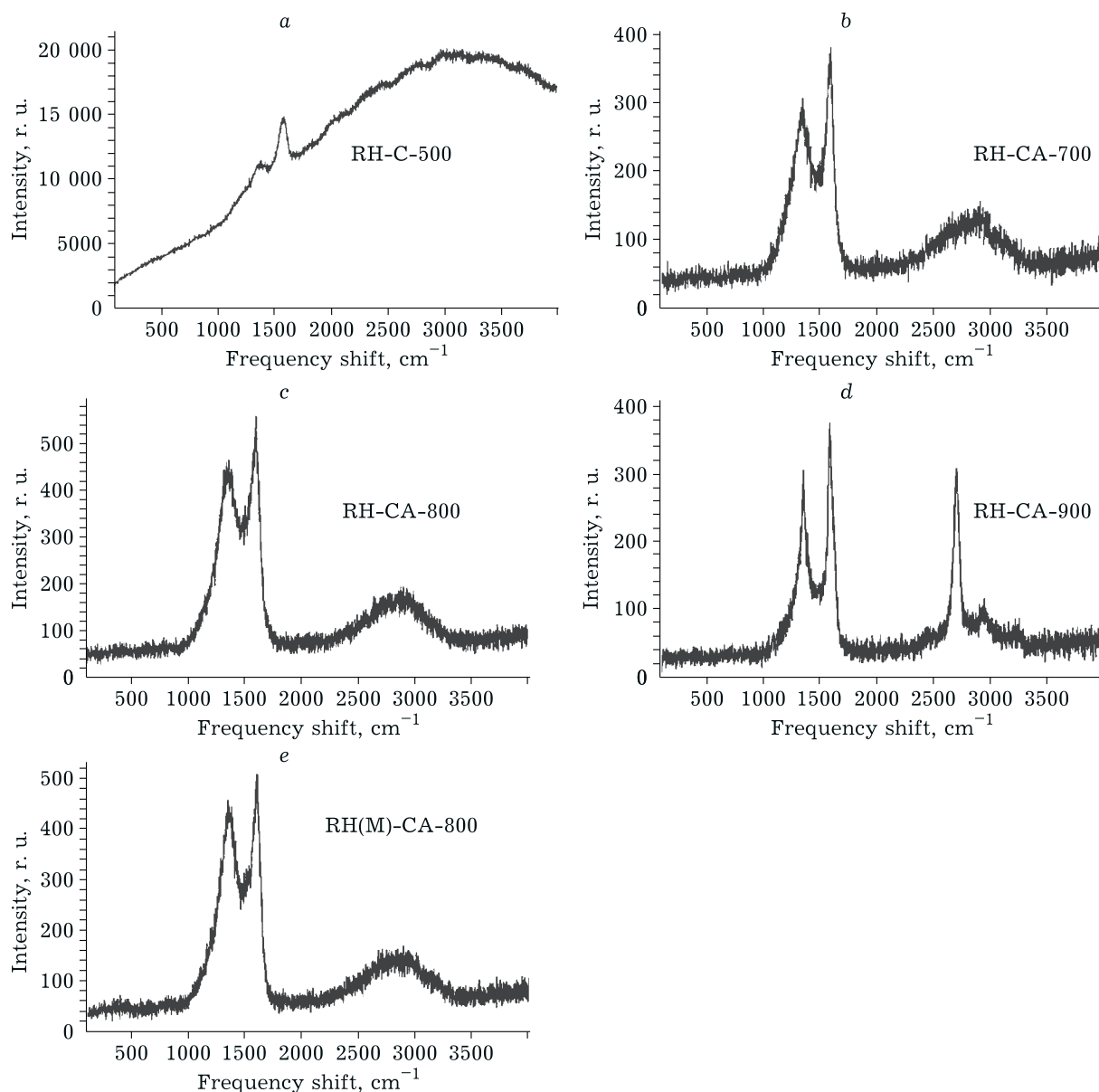


Fig. 2. Raman spectra of carbon materials based on rice husk: RH-C-500 (*a*), RH-CA-700 (*b*), RH-CA-800 (*c*), RH-CA-900 (*d*), RH(M)-CA-800 (*e*).

D3-band  $\sim 1520\text{ cm}^{-1}$  (interstitial defects outside the graphite layers, due to the formation of organic molecules, fragments or functional groups forming amorphous carbon phases);

G-band  $\sim 1585\text{ cm}^{-1}$  (vibrations of  $sp^2$  carbon atoms in graphite planes);

D2-band  $\sim 1620\text{ cm}^{-1}$  (edge defects of the  $sp^2$  graphite plane).

With an increase in activation temperature from 700 to 900 °C, the ratio of the integral intensities of D- and G-bands ( $I_D/I_G$ ), which shows the extent of structural disordering, decreases from 0.92 to 0.76, that is, the structure becomes less deficient. At 800 °C, the maximal  $I_D/I_G$  value equal to 1.05 is observed. So, it may be assumed that an increase in temperature from 700 to 800 °C leads to a substantial rearrangement of the carbon structure, followed by ordering at 900 °C. A narrow intense band at  $\sim 2700\text{ cm}^{-1}$  is detected in the Raman spectrum of RH-CA-900 sample (see Fig. 2, d), which is characteristic of graphite and other highly symmetric carbon materials with the low content of structural defects. Most probably, this phenomenon may be related to the initial stage of graphitization of the carbon material.

Additional confirmation of this assumption may be the position of the maximum of intensity (frequency shift,  $\nu$ ,  $\text{cm}^{-1}$ ) and half-widths of spectral bands ( $\Delta\nu$ ,  $\text{cm}^{-1}$ ) of the basic vibrations. The G-band in the Raman spectrum of RH-CA-700 sample may be described by the following values:  $\nu(\text{G}) = 1602\text{ cm}^{-1}$  and  $\Delta\nu(\text{G}) = 78\text{ cm}^{-1}$ . The characteristic for the D-band is:  $\nu(\text{D}) = 1354\text{ cm}^{-1}$  and  $\Delta\nu(\text{D}) = 183\text{ cm}^{-1}$ . This means that graphite-like crystals incorporated into the structure of carbonized are composed of conjugated benzoic rings having a shorter bond length in comparison with the saturated six-membered rings, which leads to the high  $\nu$  value of the G-band.

An increase in the temperature of chemical activation to 800 °C only slightly changes the spectral characteristics:  $\nu(\text{G}) = 1601\text{ cm}^{-1}$ ,  $\Delta\nu(\text{G}) = 87\text{ cm}^{-1}$ ,  $\nu(\text{D}) = 1356\text{ cm}^{-1}$ ,  $\Delta\nu(\text{D}) = 215\text{ cm}^{-1}$ . Broadening of G- and D-bands is the evidence of an increase in structural disordering: defects appear that had not been present previously in graphite-like crystallites. For this reason, the RH-CA-800 sample is characterized by the high value of the parameter  $I_D/I_G$  (1.05).

Further increase in temperature to 900 °C leads to the change of the vibrational spectrum: the bands possess the minimal width, and

the G-band shifts to the spectral region characteristic of graphite:  $\nu(\text{G}) = 1587\text{ cm}^{-1}$ ,  $\Delta\nu(\text{G}) = 43\text{ cm}^{-1}$ ,  $\nu(\text{D}) = 1353\text{ cm}^{-1}$ ,  $\Delta\nu(\text{D}) = 87\text{ cm}^{-1}$ . Thus the carbon structure of the RH-CA-900 sample is the most ordered one, with the smallest number of defects. This is the reason for a decrease in the specific surface area (see Fig. 1).

The parameters of D-band ( $\nu(\text{D}) = 1353\text{ cm}^{-1}$ ,  $\Delta\nu(\text{D}) = 176\text{ cm}^{-1}$ ) for sample RH(M)-CA-800 which was preliminarily mechanically activated differ from the parameters of the sample without mechanical activation (RH-CA-800). The characteristics of G-band ( $\nu(\text{G}) = 1601\text{ cm}^{-1}$ ,  $\Delta\nu(\text{G}) = 86\text{ cm}^{-1}$ ) are close for both samples, which means that preliminary mechanical activation has not affected the formation of the ordered phase. A decrease in the width of D-band may be a consequence of annealing some structural defects. For the RH(M)-CA-800 sample,  $I_D/I_G = 1.25$ , which means that the structure of this sample contains a larger amount of defects. This is most probably connected with an increase in the fraction of edge defects (D4-band), which appear in the Raman spectrum in the high-frequency shoulder of the G-band. An increase in the intensity of D4-band is accompanied by a decrease in the intensity of G-band, so the value of  $I_D/I_G$  increases. An increase in the amount of edge defects of graphite-like crystallites leads to an increase in the specific surface of the sample (see Fig. 1).

The CVA curves of symmetrical SC cells are shown in Fig. 3. One can see that SC cells with the electrodes based on carbonized husk RH-C-500 without chemical activation do not exhibit capacitance properties in the alkaline electrolyte and in the acid; the shapes of curves are not rectangular, and the area limited by CVA curves is insignificant. The maximal value of current at 80 mV/s does not exceed 0.6–0.7 mA (or 0.03 A/g); the capacity of electrodes at the scanning rate of 10 mV/s was 32–34 F/g, while at 80 mV/s – 4–5 F/g. For the cells with electrode materials based on the samples subjected to high-temperature chemical activation (RH-CA-700, RH-CA-800, RH-CA-900), the shape of curves is close to rectangular, especially for RH(M)-CA-800 sample that was preliminarily activated mechanically, which is characteristic of SC accumulating energy due to the double electric layer (DEL). The areas limited by CVA curves are many times larger for activated samples than for the case when non-activated carbonized rice husk is used (RH-C-500). Current densities in the cases when

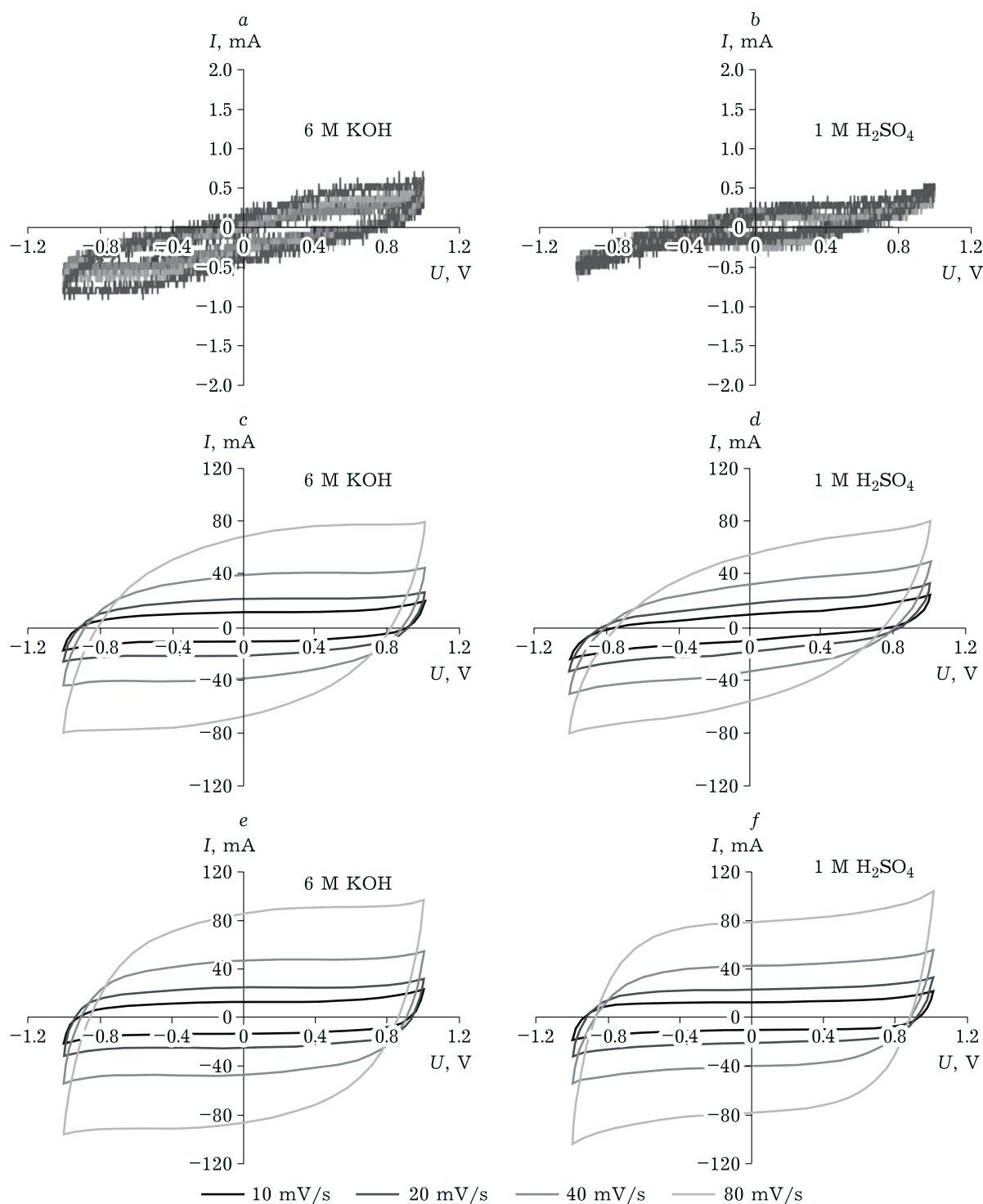


Fig. 3. CVA curves of the symmetrical supercapacitor cells in the alkaline (a, c, e) and acid (b, d, f) electrolytes. Electrode materials: a, b – RH-C-500; c, d – RH-CA-800; e, f – RH(M)-CA-800.

RH-CA-700, RH-CA-800, RH-CA-900 were used at 80 mV/s reached 4–5 A/g (calculated for the mass of two electrodes).

The dependences of specific capacitance ( $C$ ) of electrodes in symmetrical SC cells on the rate of potential scanning ( $v$ ) are shown in Fig. 4. One

can see that the highest capacity is observed when the electrode material is preliminarily ground carbonized husk subjected to chemical activation at 800 °C (RH(M)-CA-800): 491 F/g – in 6 M KOH solution, 469 F/g – in 1 M H<sub>2</sub>SO<sub>4</sub> solution.

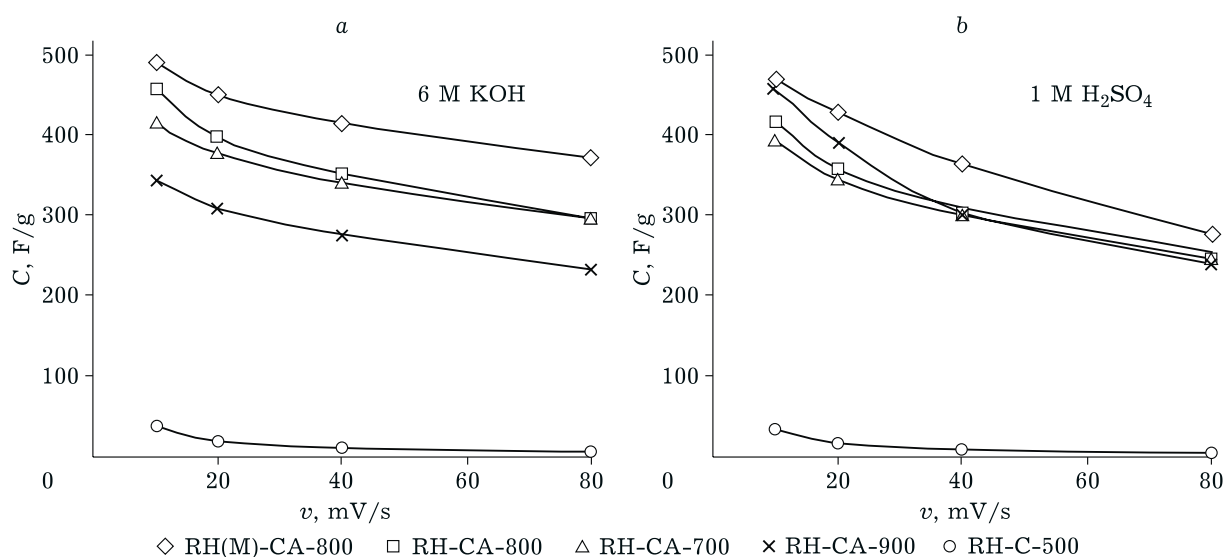


Fig. 4. Dependence of specific capacitance of electrode materials on the rate of potential scanning in the alkaline (a) and acid (b) electrolytes.

Comparing the data obtained in the studies in two electrolytes, we see that at high scanning rates somewhat higher parameters were revealed for the cell with the alkaline electrolyte (6 M KOH). Among the samples activated in the alkaline electrolyte, the smallest capacitance was observed for RH-CA-900 sample: in the acid electrolyte (1 M H<sub>2</sub>SO<sub>4</sub>) at low scanning rates (10 mV/s) the capacity of this electrode material was 458 F/g, which is comparable with the capacitance of RH(M)-CA-800. However, unlike for the latter, the shape of CVA curves is not rectangular but extended across the diagonal, and at scanning rate of 80 mV/s the capacitance of RH-CA-900 noticeably decreases to 235 F/g.

Results of the calculations carried out on the basis of the curves of galvanostatic charge-discharge are shown in Table 1.

In comparison with CVA data, relatively lower cell capacitance values calculated from discharge curves are due to higher rates of potential change,

especially for the samples with low capacitance and high internal resistance. The highest capacity and the smallest internal resistance were observed with the RH(M)-CA-800 sample used in the alkaline electrolyte. One can see that the high-temperature chemical activation of carbonized rice husk by potassium hydroxide allows a 55–95 times increase in capacitance and a 150–300 times decrease in the internal resistance in comparison with the electrode material RH-C-500.

The Nikewist diagrams and the dependences of the phase angle ( $\varphi$ ) on frequency ( $f$ ) for SC cells with the electrode materials under investigation are shown in Fig. 5. The lowest resistance is observed when carbon materials activated at 800 °C are used, especially RH(M)-CA-800 sample which was prepared by preliminary mechanical activation. Nikewist diagrams for the cells with electrodes based on RH-CA-800 and RH(M)-CA-800 samples correspond in their shape to the hodographs of SC impedance, in which the dominating

TABLE 1

Specific capacitance of the electrodes and internal resistance of supercapacitor cells calculated from the discharge curve

Sample	Specific capacitance, F/h		Internal resistance, Ohm	
	6 M KOH	1 M H <sub>2</sub> SO <sub>4</sub>	6 M KOH	1 M H <sub>2</sub> SO <sub>4</sub>
RH-C-500	3	2	963.0	971.0
RH-CA-700	167	174	5.6	5.8
RH-CA-800	193	181	3.9	4.0
RH-CA-900	175	172	4.8	6.2
RH(M)-CA-800	206	189	3.2	3.4

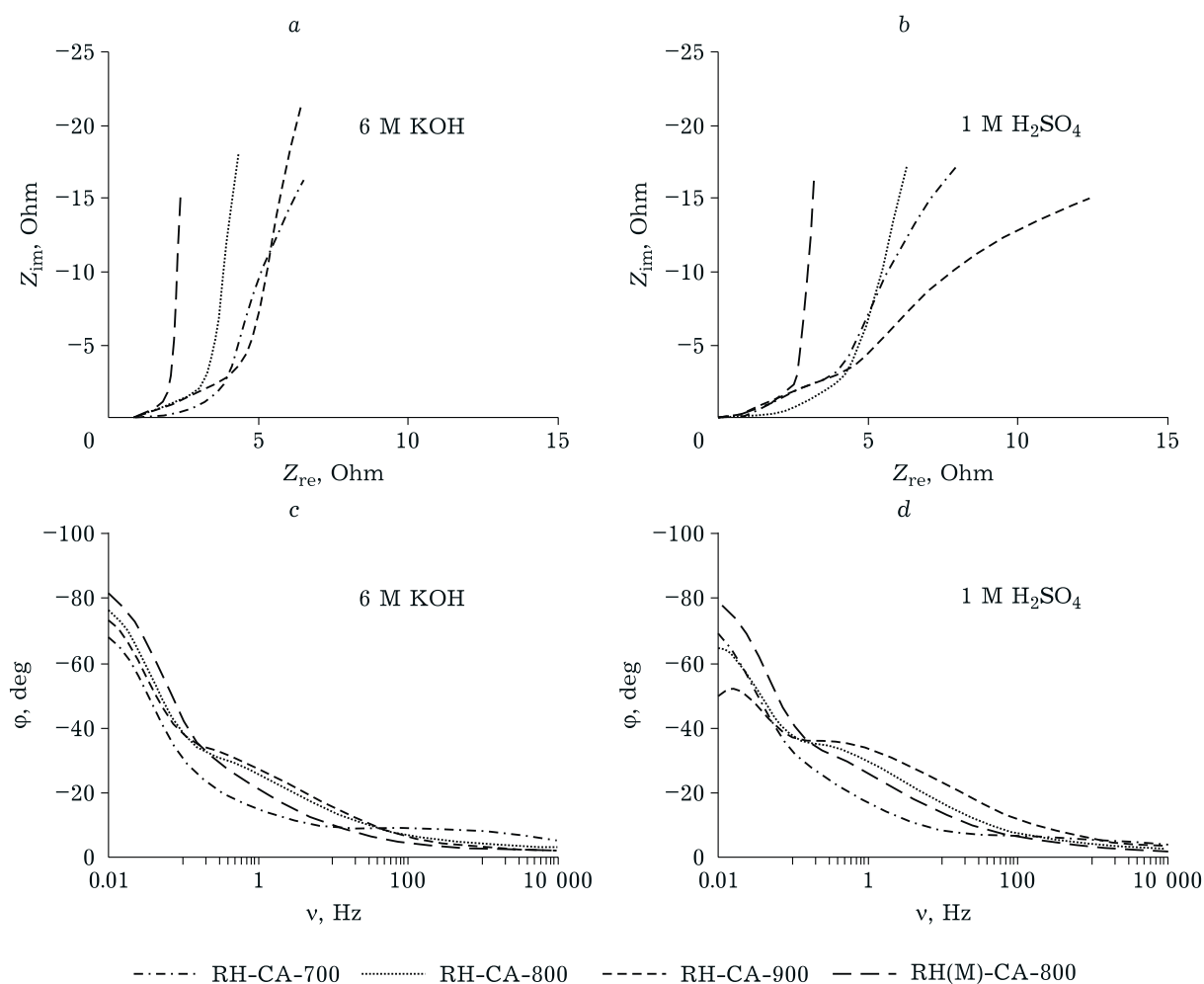


Fig. 5. Nyquist diagrams (a, b) and the dependences of phase angle ( $\varphi$ ) of supercapacitor cells on current frequency ( $\nu$ ) (c, d) in different electrolytes.

contribution into capacity is made by the DEL; for other electrode materials, a substantial increase in the active component of the impedance and a decrease in phase angle are observed with a decrease in current frequency. For chemically non-activated sample (RH-C-500, not shown in Fig. 5), the phase angle is within the range 15–25 deg, the active and reactive components of the impedance are 0.5–2 kOhm, which is in agreement with the data of CVA, galvanostatic charge-discharge and points to the low capacitance characteristics and impossibility to use non-activated rice husk as electrodes in SC. For the activated sample, the lowest active component of the impedance is observed for the sample activated at 800 °C. Additional preliminary mechanical activation of carbonized husk promotes a decrease in the active component of the impedance to 2–3 Ohm at the frequency of 0.01 Hz and an increase in phase angle to 80 deg. This is evidence that the major

contribution to capacitance is explained by charge accumulation due to DEL.

## CONCLUSION

Highly porous activated carbon materials obtained through carbonization of rice husk followed by activation with potassium hydroxide were studied with the help of Raman spectroscopy and electrochemical methods. The samples are characterized by the high specific surface (1200–2300  $m^2/g$ ) and pore volume (up to 1.03  $cm^3/g$ ), in particular micropores (up to 0.84  $cm^3/g$ ). It was established that the optimal temperature of chemical activation is 800 °C. It was determined that preliminary mechanical activation of rice husk followed by chemical activation with the help of potassium hydroxide allows a substantial increase in the specific electrical capacitance to 450–490 F/g and decrease the impedance of cells,



which is due to an increase in the concentration of defects in the structure, an increase in the specific surface area and the volume of pores, first of all micropores.

## Acknowledgements

The work was carried out with financial support from the Russian Science Foundation (Project No. 19-13-00129), using the equipment at the Shared Equipment Centre of the FRC CCC SB RAS (Kemerovo).

## REFERENCES

- Tadda M. A., Ahsan A., Shitu A., ElSergany M., Arunkumar T., Jose B., Razzaque A. M., Daud N. N. A review on activated carbon: Process, application and prospects, *Journal of Advanced Civil Engineering Practice and Research*, 2016, Vol. 2, No. 1, P. 7–13.
- Menya E., Olupot P. W., Storz H., Lubwama M., Kiros Y. Production and performance of activated carbon from rice husks for removal of natural organic matter from water: A review, *Chemical Engineering Research and Design*, 2018, Vol. 129, P. 271–296.
- Iqbal S., Khatoon H., Pandit A. H., Ahmad S. Recent development of carbon based materials for energy storage devices, *Materials Science for Energy Technologies*, 2019, Vol. 2, P. 417–428.
- Gao Z., Zhang Y., Song N., Li X. Biomass-derived renewable carbon materials for electrochemical energy storage, *Mater. Res. Lett.*, 2017, Vol. 5, No. 2, P. 69–88.
- Fic K., Platek A., Piwek J., Frackowiak E. Sustainable materials for electrochemical capacitors, *Materials Today*, 2018, Vol. 21, P. 437–454.
- Herou S., Schlee P., Jorge A. B., Titirici M. Biomass-derived electrodes for flexible supercapacitors, *Current Opinion in Green and Sustainable Chemistry*, 2018, Vol. 9, P. 18–24.
- Chen Y., Zhu Y., Wang Z., Li Y., Wang L., Ding L., Gao X., Ma Y., Guo Y. Application studies of activated carbon derived from rice husks produced by chemical-thermal process - a review, *Advances in Colloid and Interface Science*, 2011, Vol. 163, P. 39–52.
- Satayeva A. R., Korobeinyk A. V., Inglezakis V. J., Howell C. A., Mikhailovsky S. V., Jandosov J., Mansurov Z. A. Investigation of rice husk derived activated carbon for removal of nitrate contamination from water, *The Science of the Total Environment*, 2018, Vol. 630, P. 1237–1245.
- Kerimkulova A. R., Azat S., Mansurov Z. A., Tulepov M. I., Kerimkulova M. R., Imangazy A., Velasco L., Lodewyckx P., Berezovskaya I. Granular rice husk based sorbents for sorption of vapors of organic and inorganic matters, *Journal of Chemical Technology and Metallurgy*, 2019, Vol. 54, No. 3, P. 578–584.
- Seitzhanova M. A., Mansurov Z. A., Yeleuov M., Roviello V., Capua R. D. The characteristics of graphene obtained from rice husk and graphite, *Eurasian Chemico-Technological Journal*, 2019, Vol. 21, No. 2, P. 149–156.
- Gao Y., Li L., Jin Y., Wang Y., Yuan C., Wei Y., Chen G., Ge J., Lu H. Porous carbon made from rice husk as electrode material for electrochemical double layer capacitor, *Applied Energy*, 2015, Vol. 153, P. 41–47.
- Ismagilov Z. R., Shikina N. V., Andrievskaya I. P., Rudina N. A., Mansurov Z. A., Burkitbaev M. M., Biisenbaev M. A., Kurmanbekov A. A. Preparation of carbonized rice husk monoliths and modification of the porous structure by SiO<sub>2</sub> leaching, *Catalysis Today*, 2009, Vol. 147, P. 58–65.
- Liou T., Wu S. Characteristics of microporous/mesoporous carbons prepared from rice husk under base- and acid-treated conditions, *J. Hazard. Mater.*, 2009, Vol. 171, No. 1-3, P. 693–703.
- He X., Ling P., Yu M., Wang X., Zhang X., Zheng M. Rice husk-derived porous carbons with high capacitance by ZnCl<sub>2</sub> activation for supercapacitors, *Electrochim. Acta*, 2013, Vol. 105, P. 635–641.
- Liu D., Zhang W., Huang W. Effect of removing silica in rice husk for the preparation of activated carbon for supercapacitor applications, *Chinese Chemical Letters*, 2019, Vol. 30, P. 1315–1319.
- Pandolfo A. G., Hollenkamp A. F. Carbon properties and their role in supercapacitors, *Journal of Power Sources*, 2006, Vol. 157, No. 1, P. 11–27.
- Largeot C., Portet C., Chmiola J., Taberna P.-L., Gogotsi Y., Simon P. Relation between the ion size and pore size for an electric double-layer capacitor, *J. Am. Chem. Soc.*, 2008, Vol. 130, P. 2730–2731.
- Da Silva L. M., Cesar R., Moreira C. M. R., Santos J. H. M., De Souza L. G., Pires B. M., Vicentini R., Nunes W., Zanin H. Reviewing the fundamentals of supercapacitors and the difficulties involving the analysis of the electrochemical findings obtained for porous electrode materials, *Energy Storage Materials*, 2020, Vol. 27, P. 555–590.
- Zhang L., Hu X., Wang Z., Sun F., Dorrell D. G. A review of supercapacitor modeling, estimation, and applications: A control/management perspective, *Renewable and Sustainable Energy Reviews*, 2018, Vol. 81, P. 1868–1878.
- Zuliani J. E., Tong S., Jia C. Q., Kirk D. W. Contribution of surface oxygen groups to the measured capacitance of porous carbon supercapacitors, *J. Power Sources*, 2018, Vol. 395, P. 271–279.
- González A., Goikolea E., Barrena J. A., Mysyk R. Review on supercapacitors: Technologies and materials, *Renewable and Sustainable Energy Reviews*, 2016, Vol. 58, P. 1189–1206.
- Simenyuk G. Y., Puzynin A. V., Podyacheva O. Y., Salmnikov A. V., Zakharov Y. A., Ismagilov Z. R. Development of a technique and investigation of capacitance characteristics of electrode materials for supercapacitors based on nitrogen-doped carbon nanotubes, *Eurasian Chemico-Technological Journal*, 2017, Vol. 19, No. 3, P. 201–208.
- Simenyuk G. Y., Zakharov Y. A., Pavelko N. V., Dodonov V. G., Pugachev V. M., Puzynin A. V., Manina T. S., Barnakov C. N., Ismagilov Z. R. Highly porous carbon materials filled with gold and manganese oxide nanoparticles for electrochemical use, *Catalysis Today*, 2015, Vol. 249, P. 220–227.
- Manoj B. A comprehensive analysis of various structural parameters of Indian coals with the aid of advanced analytical tools, *Int. J. Coal Sci. Technol.*, 2016, Vol. 3, No. 2, P. 123–132.
- Han Y. N., Liao J. J., Bai Z. Q., Bai J., Li X., Li W. Correlation between the combustion behavior of brown coal char and its aromaticity and pore structure, *Energy & Fuels*, 2016, Vol. 30, No. 4, P. 3419–3427.
- Xu J., Bai Z., Bai J., Kong L., Lv D., Han Y., Dai X., Li W. Physico-chemical structure and combustion properties of chars derived from co-pyrolysis of lignite with direct coal liquefaction residue, *Fuel*, 2017, Vol. 187, P. 103–110.
- Nikitin A. P., Zykov I. Y., Kozlov A. P., Ismagilov Z. R. Structure of carbon sorbents produced from coal, *Coke and Chemistry*, 2018, Vol. 61, No. 12, P. 463–468.